THE JOURNAL OF BIOLOGICAL CHEMISTRY VOL. 289, NO. 28, pp. 19571–19584, July 11, 2014

Mitochondrial NLRP3 Protein Induces Reactive Oxygen Species to Promote Smad Protein Signaling and Fibrosis Independent from the Inflammasome*

Received for publication, January 16, 2014, and in revised form, May 16, 2014 Published, JBC Papers in Press, May 19, 2014, DOI 10.1074/jbc.M114.550624

Nathan A. Bracey[‡1], Benjamin Gershkovich[‡], Justin Chun[§], Akosua Vilaysane[§], H. Christopher Meijndert[‡], James R. Wright, Jr.[¶], Paul W. Fedak[‡], Paul L. Beck[§], Daniel A. Muruve[§2,3], and Henry J. Duff[‡2,4]

From the [‡]Libin Cardiovascular Institute, [§]Department of Medicine, and [¶]Department of Pathology and Laboratory Medicine, The University of Calgary, Calgary, Alberta T2N 4N1, Canada

Background: NLRP3 is a pattern recognition receptor that regulates inflammatory cytokine processing through the inflammasome.
Results: In cardiac fibroblasts, NLRP3 promotes fibrotic signaling through a novel mechanism independent from cytokine release.
Conclusion: NLRP3 displays inflammasome-independent pathways in cardiac fibroblasts and during fibrosis.
Significance: NLRP3 represents a potential direct target in fibrotic heart disease and heart failure.

Nucleotide-binding domain and leucine-rich repeat containing PYD-3 (NLRP3) is a pattern recognition receptor that is implicated in the pathogenesis of inflammation and chronic diseases. Although much is known regarding the NLRP3 inflammasome that regulates proinflammatory cytokine production in innate immune cells, the role of NLRP3 in non-professional immune cells is unclear. Here we report that NLRP3 is expressed in cardiac fibroblasts and increased during TGFβ stimulation. NLRP3-deficient cardiac fibroblasts displayed impaired differentiation and R-Smad activation in response to TGFβ. Only the central nucleotide binding domain of NLRP3 was required to augment R-Smad signaling because the N-terminal Pyrin or C-terminal leucine-rich repeat domains were dispensable. Interestingly, NLRP3 regulation of myofibroblast differentiation proceeded independently from the inflammasome, IL-1β/IL-18, or caspase 1. Instead, mitochondrially localized NLRP3 potentiated reactive oxygen species to augment R-Smad activation. *In vivo*, NLRP3-deficient mice were protected against angiotensin II-induced cardiac fibrosis with preserved cardiac architecture and reduced collagen 1. Together, these results support a distinct role for NLRP3 in non-professional immune cells independent from the inflammasome to regulate differential aspects of wound healing and chronic disease.

The mobilization of resident structural cells within organ systems during injury represents an important mechanism for initiating wound healing and repair. For example, cardiac fibroblasts differentiate into myofibroblasts during chronic tissue stress following local production of soluble stimuli such as TGFβ and angiotensin II (AngII)[5] (1). Myofibroblasts are professional wound healing cells that actively remodel the extracellular matrix, increasing the deposition of collagen and, ultimately, giving rise to tissue fibrosis, a cardinal manifestation of chronic disease (2). Profibrotic signaling induced by TGFβ proceeds following ligand binding to the membrane-bound TGF receptor I-TGF receptor II complex (3). This results in the recruitment and phosphorylation of receptor-associated Smads (R-Smad 2/3), which go on to associate with a co-Smad (Smad4), forming the functional transcription factor complex that regulates profibrotic gene expression and, ultimately, cellular phenotype (4, 5). AngII is also capable of activating fibroblasts and inducing fibrosis through R-Smads, suggesting that the Smad signaling pathway represents an important determinant of cellular fate during injury (6, 7).

NLRP3 is a member of the NLR family of intracellular pattern recognition receptors that participates in non-microbial inflammation. On activation by danger/damage associated molecular patterns, NLRP3 induces the formation of the inflammasome, a multiprotein complex that consists of the adaptor molecule apoptosis-associated speck-like protein containing a caspase recruitment domain (ASC) and the effector enzyme caspase 1 (8). When activated, caspase 1 mediates the maturation of the proinflammatory cytokines IL-1β and IL-18 for secretion by innate immune cells (9). Because inflammation plays a prominent role in chronic organ injury, the NLRP3 inflammasome and its effector cytokines have been implicated

* This work was supported by operating grants from the Alberta Heart and Stroke Foundation and Canadian Institutes for Health Research.
[1] Supported in part by a studentship award from the Alberta HEART Initiative and an MD/PhD studentship from Alberta Innovates Health Solutions.
[2] Both authors contributed equally to this work.
[3] Holder of a Tier II Canada Research Chair in Inflammation and Kidney Disease and recipient of a Clinical Senior Scholar award from Alberta Innovates Health Solutions.
[4] Holder of an Alberta Heart and Stroke Cardiovascular endowed chair. To whom correspondence should be addressed: Libin Cardiovascular Institute, The University of Calgary, HRIC, GAC 72, 3280 Hospital Dr. N.W., Calgary, AB T2N 4Z6, Canada. Tel.: 403-220-5500; Fax: 403-270-0313; E-mail: hduff@ucalgary.ca.

[5] The abbreviations used are: AngII, angiotensin II; ASC, apoptosis-associated speck-like protein containing a CARD domain; CF, cardiac fibroblast; LRR, leucine-rich repeat; ROS, reactive oxygen species; mROS, mitochondrial reactive oxygen species; NACHT, domain present in Naip, CIITA, HET-E, and TP-1.

in the pathogenesis of numerous chronic diseases (10, 11). In addition to leukocytes, NLRP3 is also expressed by a variety of non-hematopoietic cell types within solid organ systems, including the heart, although its role within these non-immune cell populations remains unclear (12, 13). We reported recently that NLRP3 in renal tubular epithelial cells regulates TGFβ signaling and epithelial-mesenchymal transition independently from the inflammasome, suggesting an alternate role for NLRP3 in regulating cellular phenotypes during injury (14). The mechanisms underlying this phenomenon and their significance during chronic tissue injury and fibrosis *in vivo*, however, have not been characterized.

Cardiac fibrosis is a common pathological feature of cardiovascular disease that occurs following virtually all injuries affecting the heart. Because NLRP3 has been shown previously to promote adverse cardiac remodeling via mechanisms that are not completely understood, we looked to further characterize the cellular and molecular roles of NLRP3 in myofibroblast differentiation and fibrosis in the context of chronic cardiac injury and disease.

EXPERIMENTAL PROCEDURES

Animal Studies

Osmotic Pumps—All experiments were performed with the approval of the Animal Care Committee at the University of Calgary, and animals were housed in a specific pathogen-free facility. Male C57BL6 mice 10–12 weeks of age were used for all studies, and $Nlrp3^{+/+}$ ($n = 7$) compared with $Nlrp3^{-/-}$ ($n = 8$) as described previously (15). For osmotic pump implantation, animals were anesthetized with isoflurane mixed with oxygen by mask inhalation, and a 1-cm incision was made with a sterile blade. Osmotic pumps (Durect Corp., Cupertino, CA) were filled with recombinant human angiotensin II (Sigma-Aldrich, 1.5 mg/kg/day) or sterile saline, implanted into the dorsum, and then the incisions were closed with an 8-0 silk suture. Mice were allowed to recover with free access to standard food and water. Serial blood pressure recordings were performed using the BP2000 Visitech Systems tail cuff apparatus.

Histology—Cryosectioned slides were blocked for 1 h in PBS containing 5% goat serum and 0.1% Triton X-100. Primary antibodies to FGF-2 and αSmooth Muscle Actin (αSMA) (Santa Cruz Biotechnology, Santa Cruz, CA) were diluted 1:200 into blocking solution and incubated overnight at 4 °C. Following washing in PBS, secondary antibodies were diluted 1:400 in blocking solution and incubated for 1 h at room temperature. Embedding and sectioning of all tissue were performed under the standard protocol by Calgary Laboratory Services (Calgary, AB, Canada), and the samples were reviewed by a pathologist blinded to the identity of the samples.

Human cardiac tissue was taken from consenting patients undergoing surgical placement of cardiac left ventricular assist devices at the Foothills Medical Centre, with an ethics protocol approved by the University of Calgary. Tissue was formalin-fixed and embedded in paraffin. Slides were deparaffinized, hydrated, and blocked in 2% goat serum, 0.5% Triton-X100, and 1% albumin for 30 min, followed by 2-h incubation with antibodies against NLRP3 (R&D Systems, catalog no. MAB 6789, 1:50), collagen 1 (catalog no. Ab34710, Abcam, 1:200), and custom-made titin (1:200). After washing in PBS, the slides were incubated with appropriate fluorescent secondary antibodies diluted 1:500 in blocking solution, mounted with Prolong Gold-containing DAPI, and visualized with a confocal laser-scanning microscope (Zeiss).

Cell Culture

Isolation of Primary Cardiac Fibroblasts—Cardiac fibroblasts were isolated as described previously (16). For murine primary culture, $Nlrp3^{+/+}$ (WT), $Nlrp3^{-/-}$, $ASC^{-/-}$, and *caspase* $1^{-/-}$ mice were sacrificed at 10–12 weeks of age, and ventricles were excised, cleaned of obvious valve and pericardial structures, and processed. Subsequent passages for all primary cardiac fibroblasts were maintained in DMEM supplemented with 10% fetal bovine serum and 100 units/ml penicillin/streptomycin.

Luciferase Assay and Transfection—Luciferase activity was determined using the Stop and Glo Dual-Luciferase assay kit (Promega) according to the protocol of the manufacturer. Briefly, luciferase activity was measured using a Monolight 3010 luminometer. The day before transfection, 293T cells were plated to 60% confluency in 24-well plates. On the day of transfection, 0.5 μg of control peGFP or pCR3-hNLRP3 constructs was mixed with 0.4 μg of pCR3-TBRII and 0.1 μg of R-Smad-activated SBE4-luciferase (firefly)/thymidine-kinase-luciferase (*Renilla*) constructs in a 10:1 ratio. The medium was changed after 4–6 h, and cells were stimulated with TGFβ (10 ng/ml) for 8 h. Firefly luciferase activity was normalized to *Renilla* luciferase, and data were expressed as fold induction over mock-treated cells.

DNA Constructs and Site-directed Mutagenesis—NLRP3 Walker-A mutant constructs were generated using the QuikChange kit according to the protocol of the manufacturer (Stratagene). The following primers were used: NLRP3, 5′GGGCGGCAGGGATTGCGGCAGCAATCCTGGCCAGGA3′ (forward) and 5′TCCTGGCCAGGATTGCTGCCGCAATCCCTGCCGCCC3′ (reverse).

Immunoblotting—Tissue samples were digested in lysis buffer (150 mM NaCl, 20 mM Tris (pH 7.5), 1 mM EDTA, and 1% Nonidet P-40) supplemented with protease inhibitor mixture (Complete Minitab, Roche) and homogenized on ice. Following SDS-PAGE, nitrocellulose membranes were blocked with 5% skim milk, and immunoblotting was performed using the following antibodies: ASC (catalog no. AL177, Adipogen), NLRP3 (catalog no. Cryo2, Adipogen), caspase 1 (catalog nos. sc514 and sc515, Santa Cruz Biotechnology), phospho-IκBα (Cell Signaling Technology), IκBα (Cell Signaling Technology), GAPDH (Santa Cruz Biotechnology), tubulin (Sigma-Aldrich), smooth muscle actin (clone 1A4, Sigma-Aldrich), phospho-Smad2 (catalog no. sc135644, Santa Cruz Biotechnology), and Smad2/3 (BD Biosciences).

Immunocytochemistry—Cells were grown on sterile glass coverslips in the presence or absence of MitoTracker Red (Invitrogen, 100 nM). The medium was removed, and cells were rinsed in sterile PBS, followed by fixation in 4% paraformaldehyde (PFA) for 20 min at 37 °C. Cells were permeabilized in PBS containing 0.1% Triton X-100 and 0.05% SDS for 5 min at room

temperature, blocked in 0.02% gelatin PBS for 15 min at room temperature, and incubated with mouse anti-NLRP3 (catalog no. Cryo2, Enzo Life Sciences, 1:50), mouse anti-Smad2/3 (BD Biosciences, 1:200), and rabbit anti-GM130 (Abcam, 1:200) in blocking solution for 1 h at room temperature. Following sequential washes in PBS, secondary fluorescent antibodies were incubated at 1:500 in blocking solution for 45 min at room temperature. After washing, slides were mounted in Prolong Gold containing DAPI (Invitrogen). Confocal images were taken using a laser-scanning microscope with LSM software (Zeiss). Images were analyzed, and quantitative data were generated for Smad2/3 nuclear translocation using Volocity software (PerkinElmer Life Sciences).

Live Cell Confocal Imaging of Reactive Oxygen Species—Primary cardiac fibroblasts (50,000 cells/plate) were seeded in sterile 35-mm tissue culture plates with glass slide bottoms on the day prior to experiments. The following day, cells were treated with 400 nM MitoTracker Green (Invitrogen) and rinsed in Hanks' balanced salt solution with calcium and magnesium in the absence of phenol red. Plates were then transferred to a prewarmed 37 °C stage, and MitoSox Red (Invitrogen) was added at final concentration of 5 μM in a 2-ml final volume. MitoTempo (Santa Cruz Biotechnology) was used as a pretreatment at 500 μM for 10–12 h, diluted into complete medium.

Flow Cytometry—Primary adult murine ventricular cardiac fibroblasts were seeded in sterile 60-mm culture dishes overnight, rinsed in saline, and loaded with MitoSox (5 μM, Invitrogen) in Hanks' balanced salt solution without phenol red at 37 °C for 10 min. Cells were then dissociated gently in 0.05% trypsin for 5 min, centrifuged at 1000 $\times$ *g*, resuspended in phosphate-buffered saline, and placed on ice. 293T cells were seeded in 24-well plates, transfected with 0.5 μg of the indicated plasmids, loaded with MitoSox, rinsed, and collected from plates in phosphate-buffered saline. All flow cytometry was performed by the flow cytometry facility at the University of Calgary Centre for Advanced Technology.

Statistics and Analysis—Statistical analyses were performed using Microsoft Excel software. The results were analyzed for statistical variance using unpaired Student's *t* test or one-way analysis of variance with post hoc tests when appropriate. Statistically significant data were considered at $p < 0.05$. Data are presented as mean ± S.D. unless specified otherwise.

RESULTS

NLRP3 Regulates Cardiac Myofibroblast Differentiation—We and others have reported that NLRP3 is expressed within non-immune cell populations in the heart during injury (12, 17). Consistent with this, we detected NLRP3, ASC, and procaspase 1 in isolated murine cardiac fibroblasts (CFs) that are common precursors to myofibroblasts (Fig. 1*A*). To begin to explore the relevance of NLRP3 in the context of cardiac fibrosis, primary human CFs were differentiated into myofibroblasts, and NLRP3 was measured by immunoblotting. Treatment with either TGFβ (10 ng/ml) or AngII (1 μM) for 24 h resulted in a significant increase in NLRP3 with an associated up-regulation of αSMA, suggesting that NLRP3 may participate in fibrotic signaling (Fig. 1*B*). To explore this possibility, we isolated primary adult murine ventricular CFs from WT and *Nlrp3*$^{-/-}$ mice and stimulated them with either AngII or TGFβ. Interestingly, *Nlrp3*$^{-/-}$ CFs displayed impaired and delayed myofibroblast differentiation with reduced αSMA, connective tissue growth factor (CTGF), and MMP9 following stimulation (Fig. 1, *C* and *D*). In addition, *Nlrp3*$^{-/-}$ CFs also showed reduced αSMA reticular fiber organization (Fig. 1*D*), further implicating NLRP3 in the regulation of CF differentiation during profibrotic stimulation.

NLRP3 Promotes R-Smad Activation and Cardiac Myofibroblast Differentiation through the NACHT Domain—Because *Nlrp3*$^{-/-}$ CFs displayed delayed responsiveness to both TGFβ and AngII, we next explore their common shared signaling pathways. Canonical TGFβ signaling occurs downstream of the TGFβ receptor I-TGFβ receptor II complex with recruitment and activation of R-Smads. AngII is also capable of signaling directly via R-Smads, and Smad-independent pathways have been described in both fibroblasts and epithelial cells downstream of AngII and TGFβ (18). To determine whether NLRP3 participates in the early/immediate profibrotic signaling response, we stimulated primary WT and *Nlrp3*$^{-/-}$ CFs with TGFβ and assessed the activation of the Smad pathway. WT CFs showed an early phosphorylation time course of Smad2 in response to TGFβ (Fig. 2*A*). In contrast, *Nlrp3*$^{-/-}$ CFs showed significantly delayed responses up to 60 min, evidenced by reduced levels of phosphorylated Smad2. Although we still observed a relative induction of Smad2 phosphorylation in *Nlrp3*$^{-/-}$ CFs, absolute values were reduced significantly when compared directly with WT cells at these early time points. Furthermore, despite impairment of the R-Smad pathway, *Nlrp3*$^{-/-}$ CFs displayed similar phospho-ERK1/2, phospho-AKT, and Smad4 levels compared with the WT during TGFβ stimulation, ruling out a general defect in signal transduction in these cells (Fig. 2, *B* and *C*). *Nlrp3*$^{-/-}$ CFs also showed a similar increase in cytosolic TGFRII during TGFβ stimulation compared with the WT, suggesting that NLRP3 does not participate in the early endocytic modulation of the TGF receptor machinery.

The impaired profibrotic R-Smad response observed in NLRP3-deficient fibroblasts is consistent with our previously described phenotypes in kidney epithelium, suggesting a general conserved pathway in diverse resident epithelial and fibroblastic cell types (14). To further define the mechanisms by which NLRP3 modulates R-Smad activation, experiments were performed to identify the essential NLRP3 structural elements underlying the observed response. Using an R-Smad-responsive luciferase reporter assay, 293T cells that do not express endogenous NLRP3 were transfected with a variety of NLR mutant constructs, and activation of the Smad-responsive SBE4-luciferase plasmid was determined after TGFβ treatment. A significant increase in R-Smad activity was observed in NLRP3-overexpressing cells compared with GFP-transfected controls (Fig. 3*A*). Interestingly, augmentation of Smad signaling was not observed with the expression of NLRP9 or NLRP10 constructs, suggesting a unique and specific role for NLRP3 among these NLRs in the TGFβ pathway.

Full-length NLRP3 is a tripartite protein containing an N-terminal pyrin domain (PYD), the central nucleotide binding

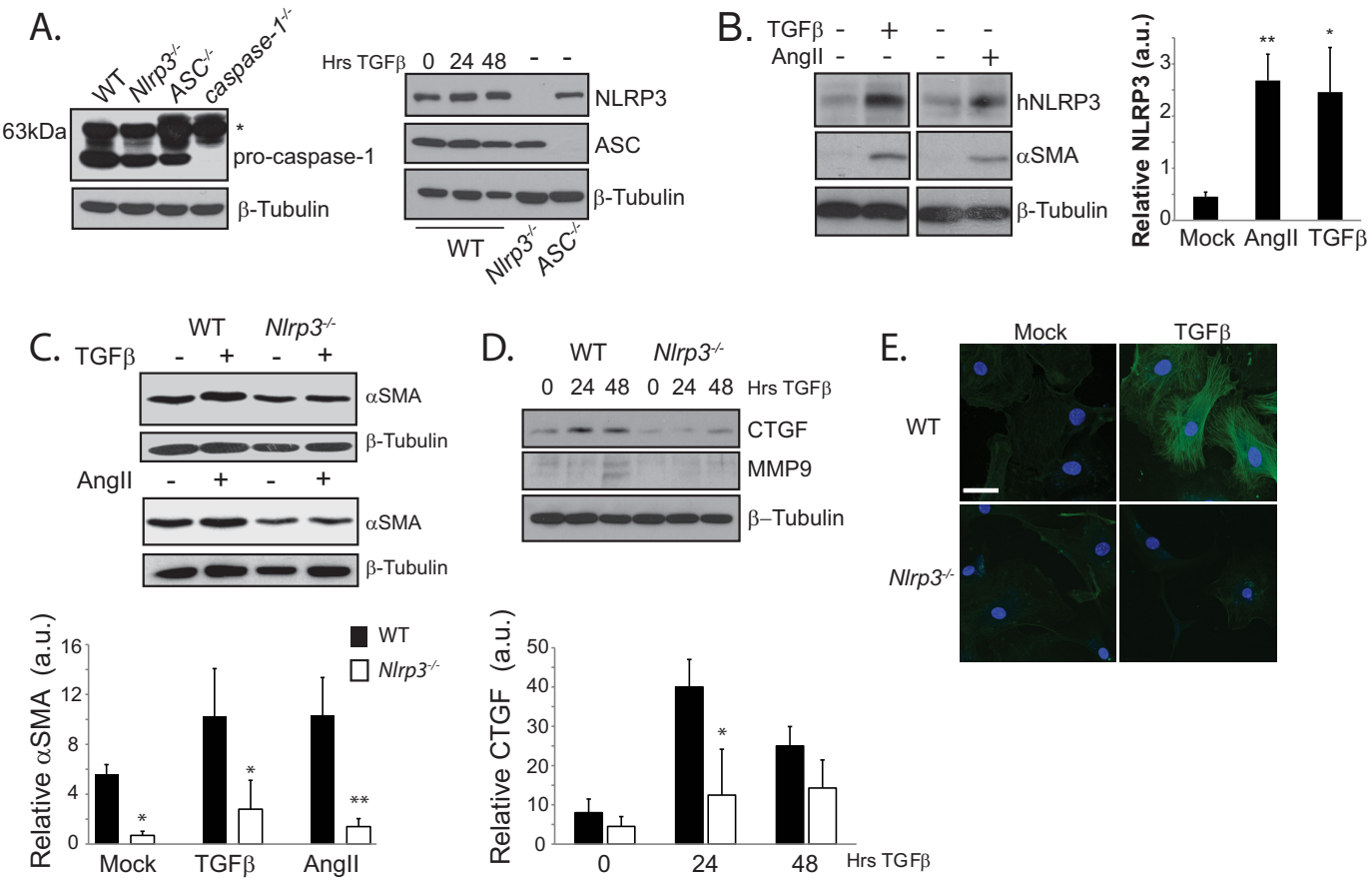

FIGURE 1. **NLRP3 regulates human cardiac myofibroblast differentiation.** *A*, immunoblotting for NLRP3, ASC, and pro-caspase 1 in murine CFs. The *asterisk* denotes a nonspecific band present at 63kDa. *B*, immunoblotting and semiquantitative analysis for NLRP3 and αSMA in human CFs (*hNLRP3*) stimulated for 24 h with TGFβ (10 ng/ml) or AngII (1 μM). *a.u.*, arbitrary units. *, $p < 0.05$; **, $p < 0.01$. *C* and *D*, immunoblotting for CTGF, MMP9, and αSMA in WT and *Nlrp3*$^{-/-}$ CFs following stimulation with TGFβ or AngII ($n = 4$). *, $p < 0.05$; **, $p < 0.01$. *E*, confocal fluorescent immunocytochemistry of αSMA in WT and *Nlrp3*$^{-/-}$ CFs following 24-h stimulation with TGFβ. *Scale bar* = 10 μm.

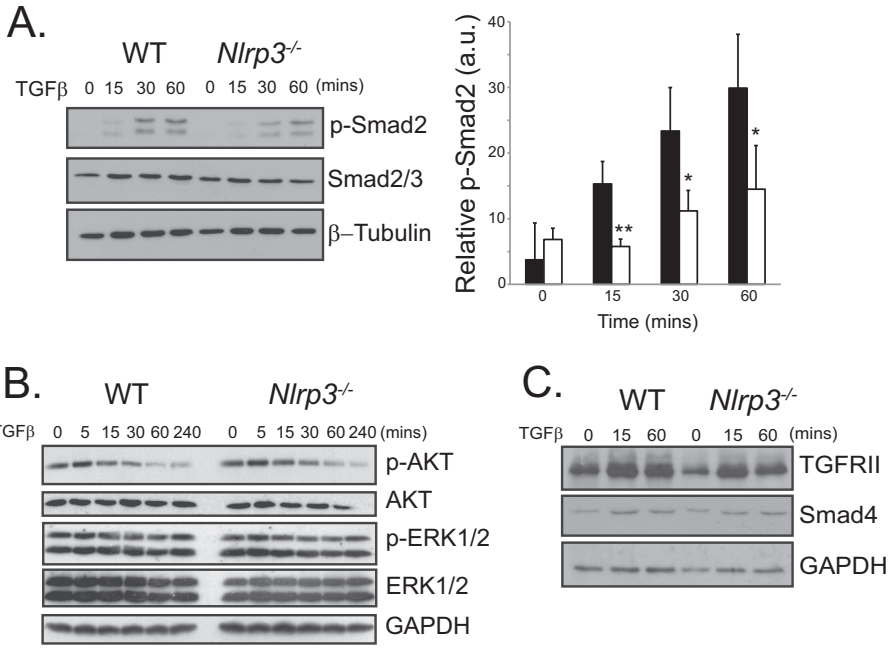

FIGURE 2. **NLRP3 regulates Smad signaling.** *A*, immunoblotting and semiquantitative analysis for phospho-Smad2 (*p-Smad2*) in TGFβ-stimulated WT and *Nlrp3*$^{-/-}$ CFs for the indicated time points ($n = 4$). *, $p < 0.05$; **, $p < 0.01$. *B* and *C*, immunoblotting for phospho-ERK1/2 (*p-ERK1/2*), phospho-AKT (*p-AKT*), TGFRII, and Smad4 in WT and *Nlrp3*$^{-/-}$ CFs stimulated with TGFβ at the indicated time points.

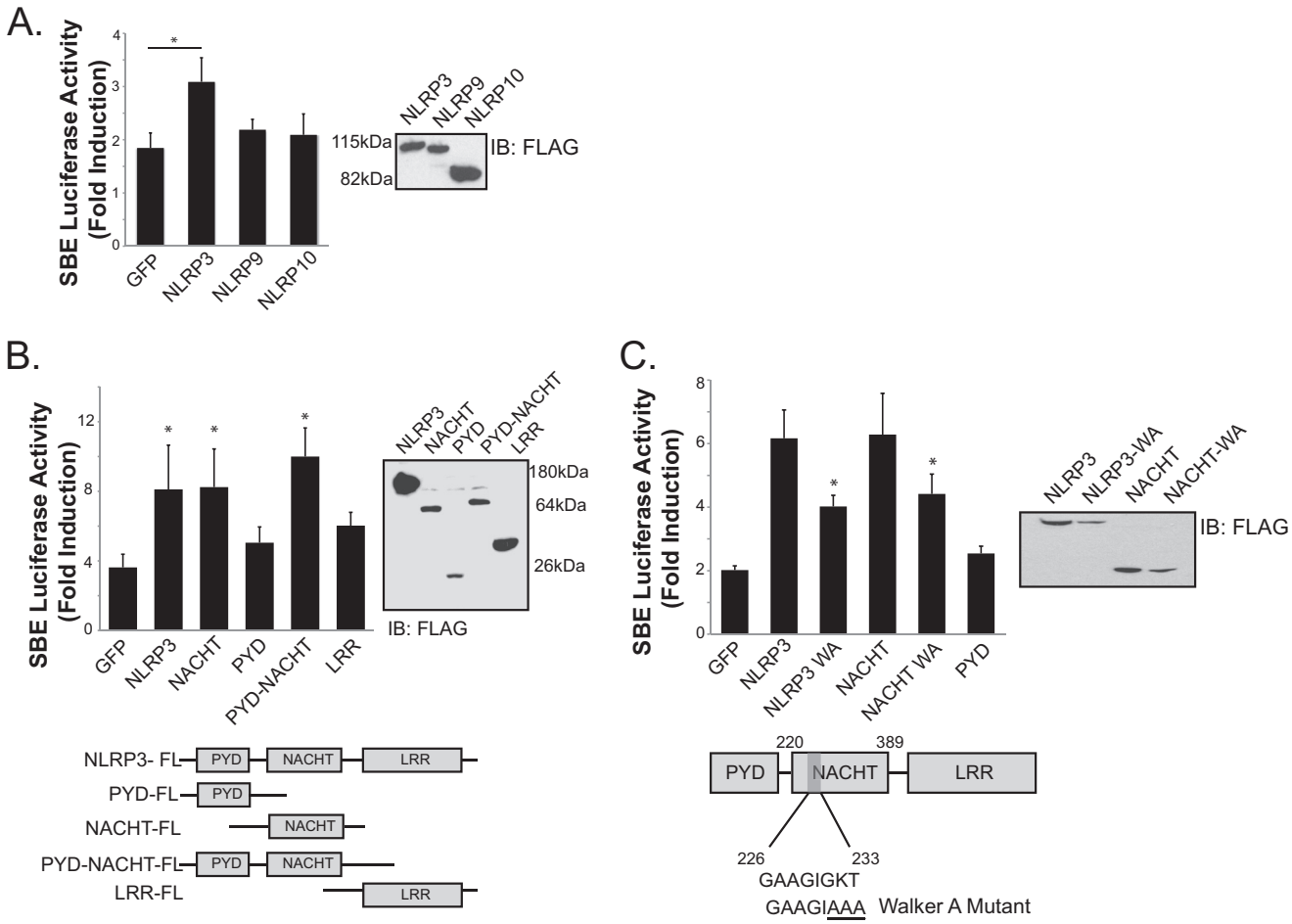

FIGURE 3. **The NLRP3 NACHT domain is required for promotion of Smad signaling.** *A*, luciferase assay and expression of FLAG-tagged NLRP3, NLRP9, and NLRP10 constructs with the SBE4-luciferase reporter in 293T cells transfected with control GFP or NLRs. *IB*, immunoblot. *B*, luciferase assay in 293T cells transfected with control GFP, NLRP3, NACHT, PYD, PYD-NACHT, or LRR constructs. Data are expressed as fold induction of luciferase activity following TGFβ stimulation (10 ng/ml) compared with mock-treated cells ($n = 3$). *, $p < 0.05$ *versus* GFP. *C*, structure and expression of the NLRP3 Walker A (*WA*) mutation in full-length NLRP3 and NACHT constructs. SBE4-luciferase assay with control GFP, NLRP3, NLRP3 Walker A mutant, NACHT, NACHT Walker A mutant, or PYD constructs ($n = 3$). *, $p < 0.05$ *versus* NLRP3.

domain (NACHT), and a C-terminal leucine-rich repeat (LRR) domain. To determine which specific structural elements are required to augment Smad signaling, NLRP3 domain mutants, including NACHT, PYD-NACHT, LRR, or PYD constructs, were employed. Compared with control GFP-transfected cells, only plasmids carrying the NACHT domain enhanced Smad activity (Fig. 3*B*). PYD- and LRR-only constructs were dispensable and did not increase Smad-dependent luciferase activity, whereas NACHT and NACHT-PYD both increased Smad activity similar to full-length NLRP3, demonstrating a critical function for the NACHT domain in NLRP3-mediated fibrotic signal transduction.

All NLRP proteins contain the conserved NACHT domain responsible for ATP coordination and hydrolysis (19). The consensus Walker A motif, characterized by G*XXXX*GK(T/S), has been shown to be critical in ATP binding, formation of the inflammasome, and IL-1β processing in macrophages (20). To determine whether the NLRP3 NACHT Walker A site was also necessary to modulate Smad activation, we created ATP-binding defective NLRP3 mutants (Fig. 3*C*). Mutation of Gly-231, Lys-232, and Thr-233 to alanine residues resulted in reduced Smad activation in both full-length NLRP3 and NLRP3-NACHT constructs, indicating a requirement for ATP/dATP binding in NLRP3-dependent Smad activation in response to TGFβ.

NLRP3 Regulates Myofibroblast Differentiation and R-Smad Signaling Independent of the Inflammasome—The previous experiments identify a role for NLRP3 in TGFβ-induced R-Smad activation and CF differentiation. Previous reports have found that IL-1β induces fibrosis and plays a significant role in cardiac injury (21–23). Given that cardiac fibroblasts express all necessary inflammasome components, the involvement of NLRP3 in fibrotic signaling could occur downstream of the inflammasome-regulated cytokines IL-1β or IL-18. Alternatively, NLRP3 could also function in an inflammasome-independent role, as suggested recently by animal models of heart and kidney injury (14, 24, 25). To address these issues directly, WT CFs were stimulated for 24 and 48 h with TGFβ and assessed for conventional inflammasome activation by immunoblotting. Surprisingly, we did not detect caspase 1 processing in CFs following TGFβ treatment, as evidenced by the absence of the 10-kDa, cleaved caspase 1 band (Fig. 4*A*). Moreover, stimulation of murine CFs with AngII or TGFβ did not induce the up-regulation or secretion of active IL-1β (Fig. 4*B*). Unlike

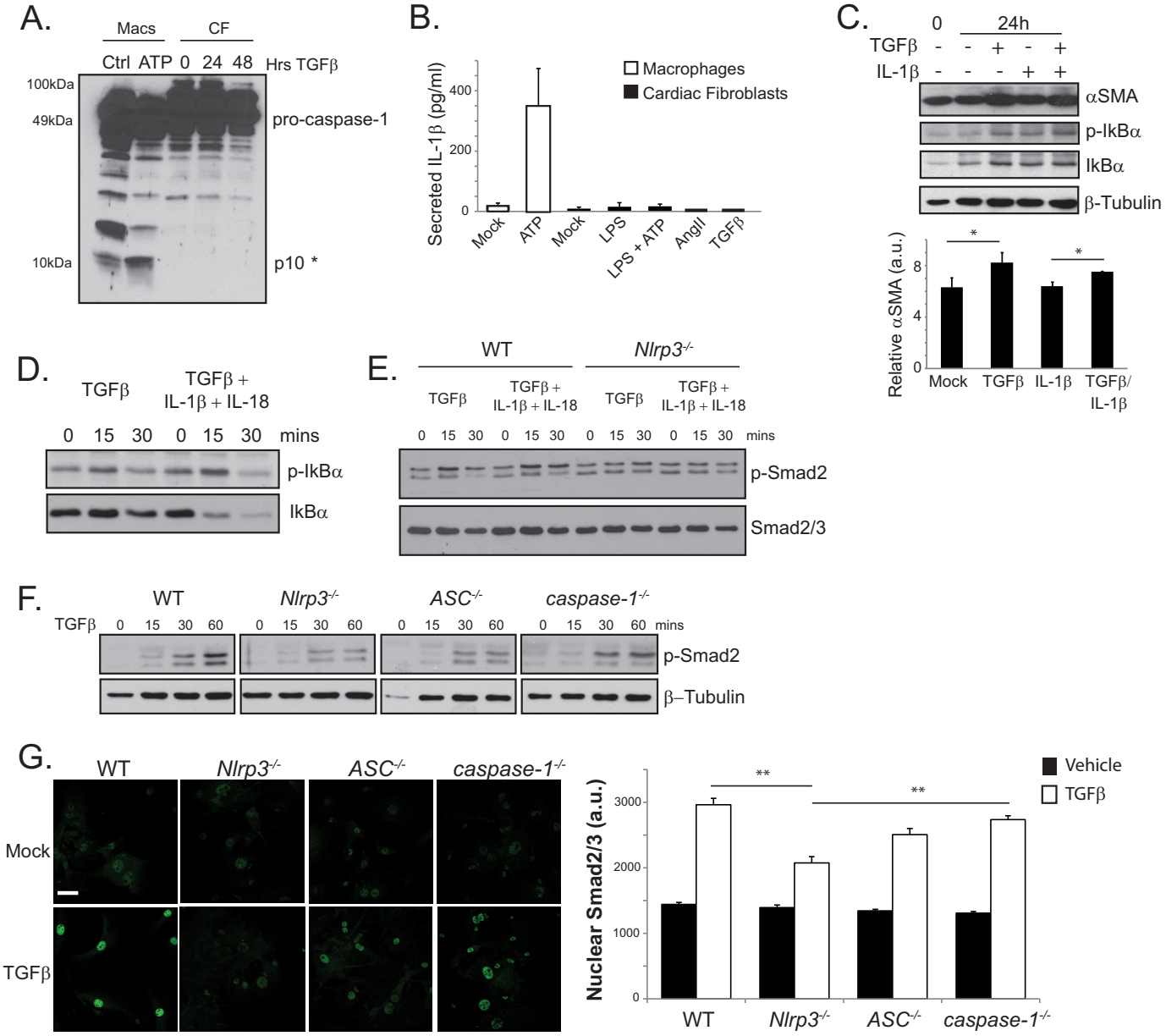

FIGURE 4. **Inflammasome independence of NLRP3 in TGFβ-induced Smad signaling.** *A*, immunoblotting for caspase 1 processing in WT CFs stimulated for 24 and 48 h with TGFβ. Primary murine peritoneal macrophages (*Macs*) primed with LPS and stimulated with 5 mM ATP for 1 h served as a positive control (*Ctrl*). The *asterisk* denotes the cleaved caspase 1 p10 band. *B*, IL-1β in supernatants from WT CFs primed with LPS (10 ng/ml) followed by ATP (5 mM) or stimulated with AngII or TGFβ. *C*, immunoblotting and semiquantitative analysis for αSMA and phospho-IκBα (*p-IκBα*) in fibroblasts stimulated with TGFβ, IL-1β (1 ng/ml), or both ($n = 3$). *a.u.*, arbitrary units. *, $p < 0.05$. *D* and *E*, immunoblotting for phospho-IκBα in *Nlrp3*$^{-/-}$ cardiac fibroblasts and phospho-Smad2 (*p-Smad2*) in WT and *Nlrp3*$^{-/-}$ CFs stimulated with TGFβ, IL-1β/IL-18 (1 ng/ml and 10 ng/ml, respectively), or all three. *F*, immunoblot for phospho-Smad2 in WT, *Nlrp3*$^{-/-}$, *ASC*$^{-/-}$, and *caspase 1*$^{-/-}$ CFs stimulated with TGFβ. *G*, confocal immunofluorescence and quantification of nuclear Smad2/3 in WT, *Nlrp3*$^{-/-}$, *ASC*$^{-/-}$, and *caspase 1*$^{-/-}$ CFs stimulated with TGFβ for 15 min. **, $p < 0.01$; $n > 30$ cells in at least four fields of view. *Error bars* indicate mean ± S.E. *Scale bar* = 40 μm.

murine peritoneal macrophages, we did not detect IL-1β secretion in CFs primed with the TLR4 ligand LPS or following subsequent stimulation with 5 mM ATP, suggesting alternative roles for NLRP3 in CF differentiation distinct from cytokine release. Despite these results, local cytokine secretion could, theoretically, still impact cardiac fibroblasts via low-level effects below the threshold of detection limits. To further rule out inflammasome-derived cytokine products as mediators of cardiac myofibroblast differentiation, fibroblasts were treated with IL-1β (1 ng/ml), TGFβ (10 ng/ml), or both cytokines (Fig. 4*C*). As anticipated, both TGFβ and IL-1β activated NFκB signaling, as evidenced by increased phosphorylation of IκBα. However, only TGFβ robustly increased αSMA following 24 h of stimulation. To directly address the relevance of the inflammasome in NLRP3 regulation of TGFβ signaling, we stimulated WT and *Nlrp3*$^{-/-}$ CFs with TGFβ alone or TGFβ plus IL-1β and IL-18 and measured Smad2 phosphorylation (Fig. 4, *D* and *E*). The addition of inflammasome-dependent cytokines to *Nlrp3*$^{-/-}$ cells still induced IκBα phosphorylation but did not rescue the Smad2 response, further indicating that NLRP3 regulation of TGFβ signaling occurs independently from the inflammasome and its downstream elements. Finally, to assess

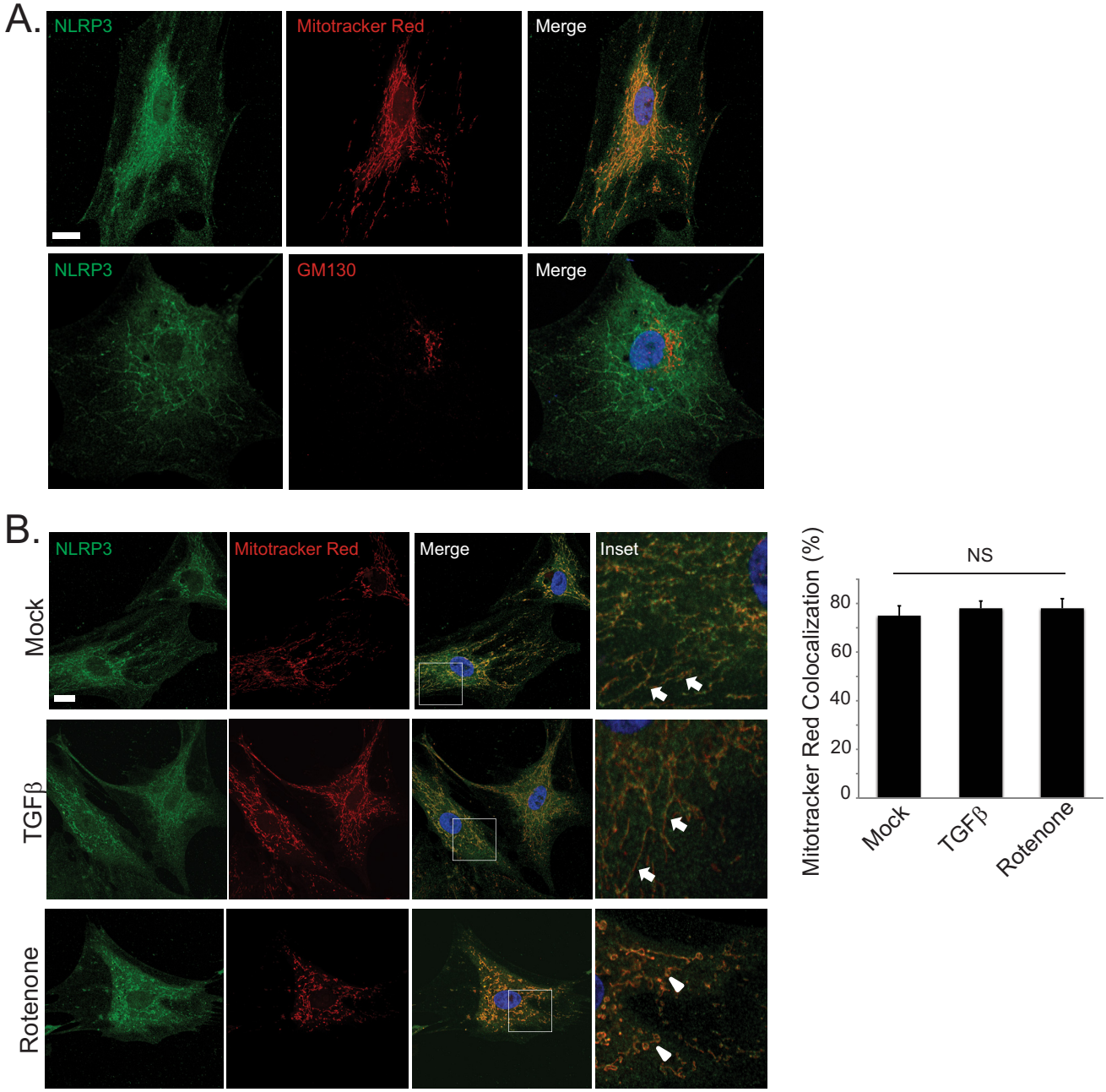

FIGURE 5. **Mitochondrial localization of endogenous NLRP3 in human cardiac fibroblasts.** *A*, confocal fluorescent immunocytochemistry for endogenous NLRP3 and MitoTracker Red (*top row*) or the cis-Golgi marker GM130 (*bottom row*) in unstimulated human CFs. *Scale bar* = 20 μm. *B*, confocal fluorescent immunocytochemistry for endogenous NLRP3 and MitoTracker Red in human CFs stimulated with TGFβ for 24 h or rotenone (10 μM) for 6 h. *Solid arrows* are directed at mitochondria with a linear morphology, and *arrowheads* are directed at mitochondria with a fragmented morphology. *Scale bar* = 20 μm. *NS*, not significant.

the relevance of other inflammasome-related proteins, CFs were isolated from WT, *Nlrp3*$^{-/-}$, *ASC*$^{-/-}$, and *caspase 1*$^{-/-}$ mice and stimulated with TGFβ. Although *Nlrp3*$^{-/-}$ cells consistently showed delayed Smad2 responsiveness to TGFβ, *caspase-1*$^{-/-}$ (also *caspase 11*$^{-/-}$) CFs responded similar to the WT (Fig. 4*F*) (26). *ASC*$^{-/-}$ cells responded as an intermediary phenotype, as described previously in kidney epithelium (20). We observed a similar pattern of Smad2/3 nuclear accumulation following early TGFβ stimulation in WT and *caspase 1*$^{-/-}$ CFs, whereas *Nlrp3*$^{-/-}$ cells displayed a significantly impaired R-Smad responses, and *ASC*$^{-/-}$ were again intermediate (Fig. 4*G*). Taken together, these results show that the involvement of NLRP3 in TGFβ-induced R-Smad phosphorylation, nuclear accumulation, and myofibroblast differentiation proceeds mechanistically independently from caspase 1 or the inflammasome-dependent cytokines IL-1β and IL-18.

NLRP3 Localizes to Mitochondria in Human Cardiac Fibroblasts and Regulates Mitochondrial ROS Production—The localization of NLRP3 during inflammasome activation to mitochondria is well documented in professional immune cells (27). NLRP3 has also been shown to participate in inflammasome signaling via detection of mitochondrial ROS follow-

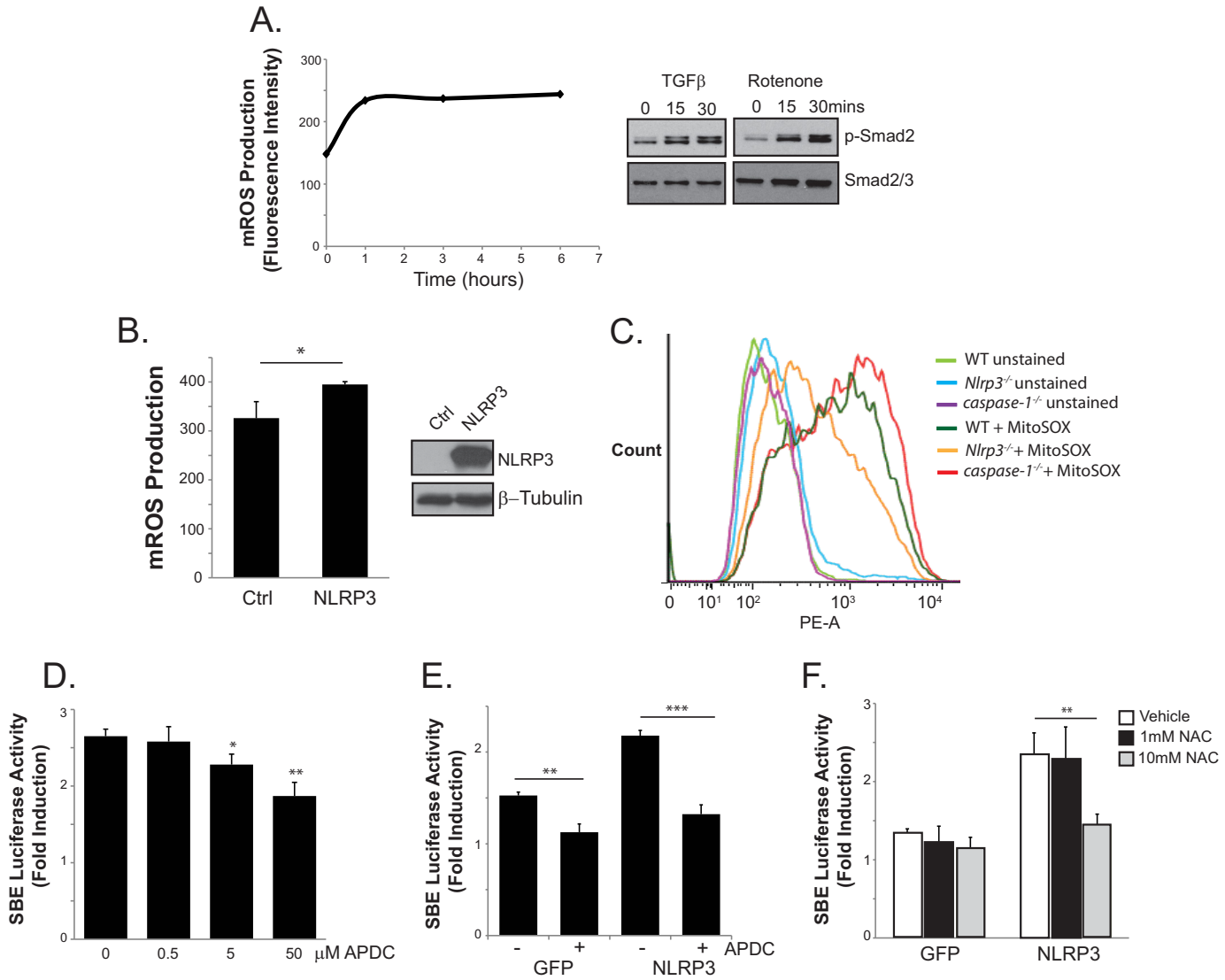

FIGURE 6. **Role of mitochondrial ROS in NLRP3-mediated Smad signaling.** *A*, *left panel*, mROS measurements on MitoSox-loaded (5 μM) 293T cells transfected with the TGF type II receptor, stimulated with TGFβ for the indicated times, and subjected to flow cytometry. Data are expressed as mean fluorescence intensity units. *Right panel*, immunoblot for phosphorylated Smad2 (*p-Smad2*) in human CFs treated with either TGFβ or rotenone (10 μM). *B*, flow cytometry quantification of MitoSox-loaded (5 μM) 293T cells transfected with either a control plasmid (*Ctrl*) or NLRP3. *, $p < 0.05$; $n = 3$. *C*, flow cytometry on control and MitoSox-loaded WT, *Nlrp3*$^{-/-}$, and *caspase 1*$^{-/-}$ CFs. *D* and *E*, luciferase assay with SBE4-luciferase reporter in 293T cells transfected with NLRP3 and stimulated with TGFβ in the presence of increasing concentrations of aminopyrrolidine-2,4- dicarboxylate (*APDC*, 0–50 μM). $n = 3$; *, $p < 0.05$; **, $p < 0.01$; ***, $p < 0.001$. *F*, luciferase assay comparing control GFP- *versus* NLRP3-transfected 293T cells stimulated with TGFβ in the presence of 0, 1, or 10 mM *N*-acetylcysteine (*NAC*). $n = 3$; **, $p < 0.01$.

ing cellular stress (28). Given its apparent role in modulating TGFβ signaling, we next looked to assess the subcellular localization patterns of NLRP3 in fibroblasts. In human CFs, endogenous NLRP3 localized primarily to mitochondria but not to the Golgi or nuclear structures (Fig. 5*A*). Interestingly, we did not observe a significant translocation of NLRP3 during myofibroblast differentiation (Fig. 5*B*). Stimulation of human CFs with TGFβ resulted in a similar degree of colocalization with MitoTracker Red compared with baseline, unstimulated conditions. Moreover, destabilization of mitochondria with the complex 1 electron transport chain inhibitor rotenone (10 μM) resulted in fragmented mitochondrial morphology but, again, did not significantly alter NLRP3 localization, suggesting a potentially intrinsic role for NLRP3 at the mitochondria.

Fibroblasts and epithelial cells have been well described to utilize mitochondrial ROS (mROS) as second messengers to facilitate diverse signal transduction pathways (29). In particular, TGFβ has been reported to require mROS for optimal differentiation of myofibroblasts (30). Because mROS have also been shown extensively to activate NLRP3-dependent cytokine production and caspase 1 cleavage in macrophages, we next looked to explore the role of mROS in R-Smad signaling. Consistent with previous findings, treatment of TGFRII-expressing 293T cells with TGFβ resulted in an early induction time course of mROS when assessed by flow cytometry (Fig. 6*A*). The stimulation of human CFs with rotenone (10 μM) also resulted in the early phosphorylation of Smad2, confirming the importance of ROS in TGFβ signaling. A connection between NLRP3 and

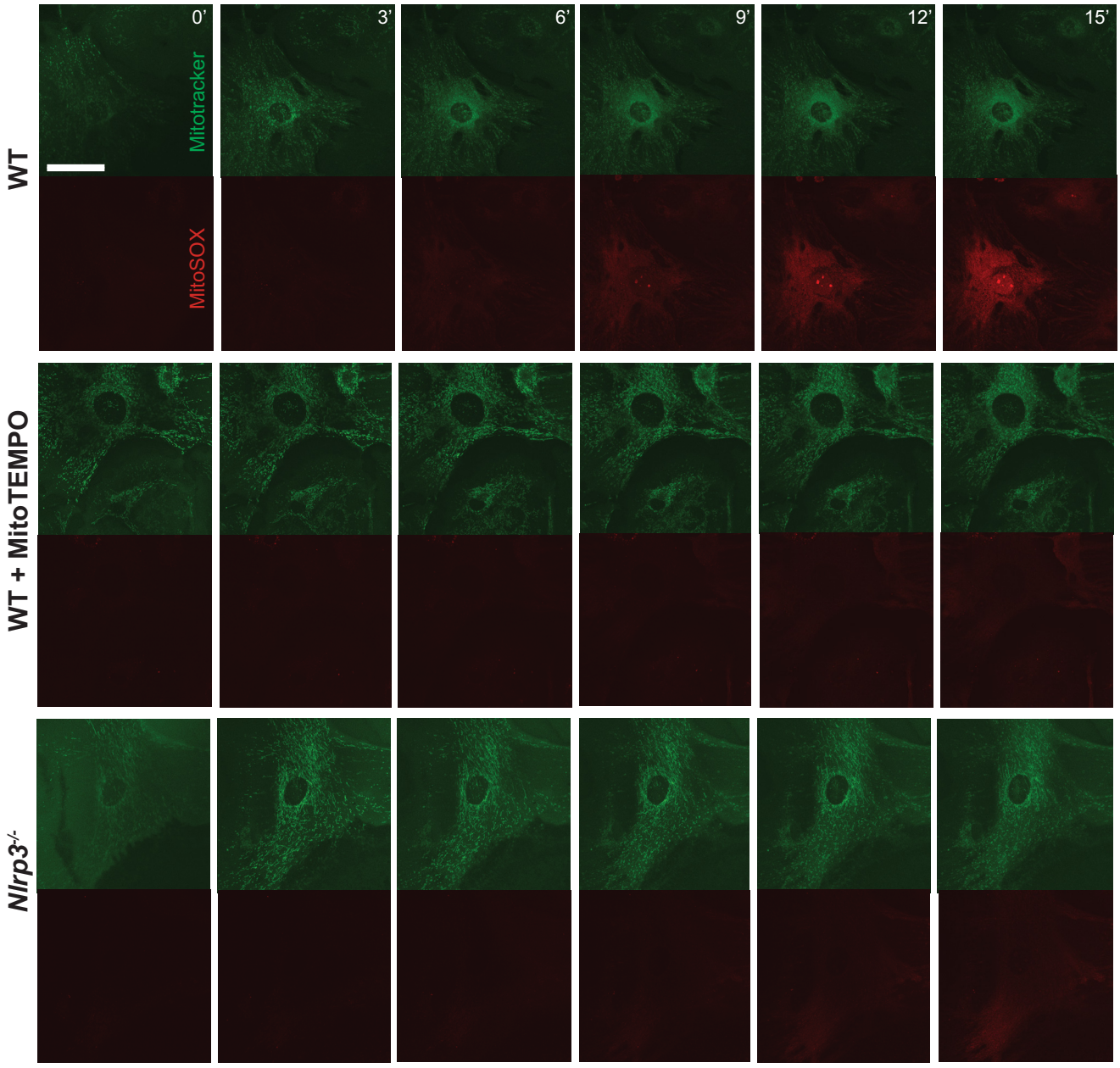

FIGURE 7. **Live cell imaging of mROS in WT and *Nlrp3*$^{-/-}$ CF.** WT and *Nlrp3*$^{-/-}$ CFs were preloaded with MitoTracker Green (400 nM, 15 min), and MitoSox (5 μM) was added at time 0 for mROS visualization by confocal imaging. WT cells were pretreated for 8 h in MitoTempo (400 mM) prior to live cell imaging. *Scale bar* = 40 μm.

ROS in the TGFβ induction of R-Smads could operate similar to previous reports documenting ROS-mediated activation of the NLRP3 inflammasome, with NLRP3 as a sensor for reactive intermediates. Alternatively, NLRP3 could have uncharacterized roles in mitochondrial function, given its persistent localization pattern in CFs. To resolve this, we examined the relative degree of mROS production in control GFP- and NLRP3-expressing cells loaded with the mitochondrial ROS fluorescent indicator MitoSox using flow cytometry. Surprisingly, the overexpression of NLRP3 in 293T cells resulted in significantly increased mROS compared with controls (Fig. 6*B*). To further explore these results, isolated WT, *caspase 1*$^{-/-}$, and *Nlrp3*$^{-/-}$ CFs were loaded with MitoSox, and mROS was quantified with flow cytometry. Although WT and *caspase 1*$^{-/-}$ CFs showed similar profiles, *Nlrp3*$^{-/-}$ cells displayed reduced mROS, again consistent with an inflammasome-independent mechanism (Fig. 6*C*).

The previous studies point to an additional and novel role for NLRP3 in the regulation of basal mROS levels, in contrast to functions as a ROS sensor described earlier. To specifically test whether antagonizing ROS could also impact NLRP3-dependent R-Smad signaling, 293T cells were transfected with NLRP3 along with the SBE4-luciferase construct, and the TGFβ-induced Smad response was measured in the presence of the general ROS inhibitor aminopyrrolidine-2,4-dicarboxylate, which has been shown previously to antagonize mROS-induced inflammasome activation (28). We observed a dose-dependent reduction in NLRP3-mediated Smad activity with

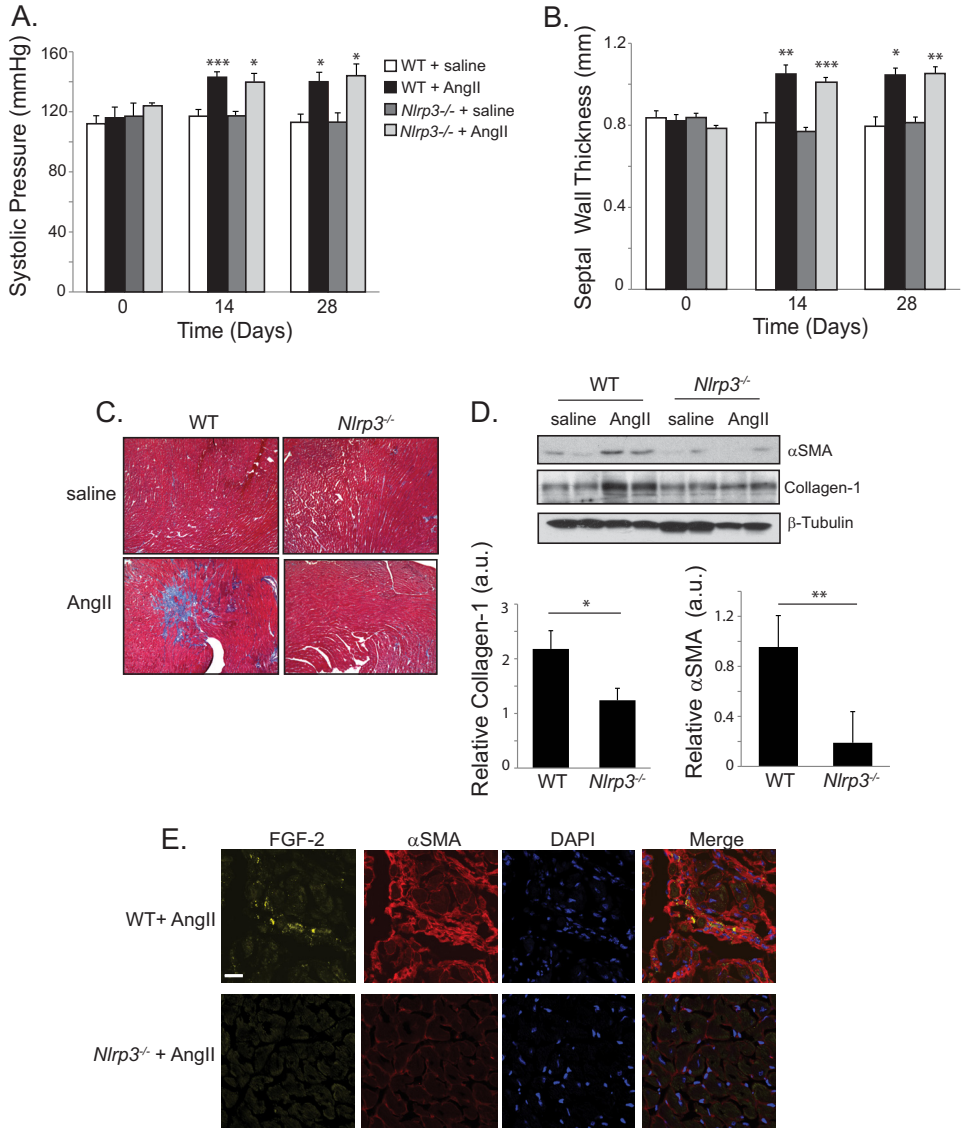

FIGURE 8. **NLRP3 regulates AngII-induced cardiac fibrosis *in vivo*.** *A* and *B*, systolic blood pressure and septal wall thickness from WT and *Nlrp3*$^{-/-}$ mice treated with saline ($n = 4$) or AngII (1.5 mg/kg/day, $n = 7$ WT, $n = 8$ *Nlrp3*$^{-/-}$). *, $p < 0.05$; **, $p < 0.01$; ***, $p < 0.001$. *C*, Masson trichrome stain of left ventricular tissue taken at 28 days following saline or AngII infusion in WT and *Nlrp3*$^{-/-}$ mice. *D*, representative immunoblot and semiquantitative analysis for αSMA and collagen 1 in ventricular cardiac tissue taken from WT and *Nlrp3*$^{-/-}$ mice at 28 days following AngII or saline ($n = 7$ WT, $n = 8$ *Nlrp3*$^{-/-}$). *a.u.*, arbitrary units. *, $p < 0.05$; **, $p < 0.01$. *E*, confocal fluorescent immunohistochemistry showing localization of αSMA and FGF-2 in ventricular tissue from AngII-treated WT and *Nlrp3*$^{-/-}$ mice. *Scale bar* = 20 μm.

increasing concentrations of aminopyrrolidine-2,4-dicarboxylate (Fig. 6, *D* and *E*). A similar response was seen in the presence of increasing concentrations of *N*-acetylcysteine (*NAC*, Fig. 6*F*). Although the blockade of ROS also reduced Smad activity in control GFP cells, the effect was significantly more pronounced in NLRP3-overexpressing cells, supporting the premise that NLRP3 exerts its effects on TGFβ signaling through the induction of mROS. To further determine the importance of these pathways in primary cells, we next looked to directly visualize differences in mROS production in CFs. Live cell imaging was performed in isolated WT and *Nlrp3*$^{-/-}$ CFs loaded with MitoTracker green and MitoSox (Fig. 7). WT CFs showed a time-dependent increase in MitoSox fluorescence intensity, which was abrogated by pretreatment with the mROS inhibitor MitoTempo. Consistent with our results using flow cytometry, live *Nlrp3*$^{-/-}$ CFs again displayed reduced mROS intensity compared with the WT, further supporting a role for NLRP3 in the regulation of mitochondrial ROS production. Collectively, these results indicate that NLRP3 operates at the mitochondria in CFs to regulate the absolute degree of mROS, which acts upstream of R-Smads to modulate TGFβ signaling and cellular differentiation.

NLRP3 Regulates Cardiac Fibrosis and Myofibroblast Differentiation in Vivo—Given the requirements for NLRP3 in cardiac myofibroblast differentiation, mROS production, and Smad signaling, we next sought to assess its relevance in the development of cardiac fibrosis using a mouse model of hypertensive disease. Infusion of AngII in mice has been well characterized to proceed through TGFβ-dependent mechanisms with the development of fibrotic lesions (31). AngII was administered to WT and *Nlrp3*$^{-/-}$ mice for 28 days, and the cardiovascular structure was assessed by blood pressure monitoring and echocardiographic assessment. AngII infusion resulted in significantly elevated blood pressure in

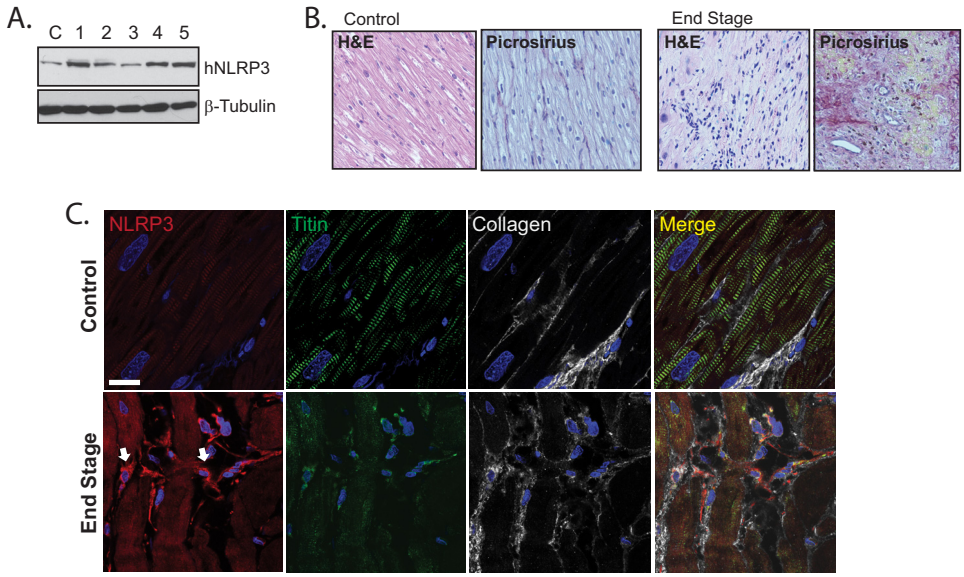

FIGURE 9. **NLRP3 expression and localization in human heart disease.** *A*, immunoblotting for hNLRP3 in human left ventricular myocardium from a control (*C*) and five patients with end-stage heart disease. *B*, H&E and picrosirius red staining for fibrosis in control tissue from patients without significant disease and left ventricular tissue from patients with end-stage heart disease. *C*, confocal fluorescent immunohistochemistry of human control samples and left ventricular heart failure tissue costained for collagen 1, NLRP3, and titin. *Arrows* are directed at NLRP3-expressing interstitial cells. *Scale bars* = 20 μm.

WT and *Nlrp3*$^{-/-}$ mice compared with saline-treated animals (Fig. 8*A*). AngII-treated mice developed moderate systolic hypertension within 1 week that persisted throughout the course of the 28-day infusion. Moreover, both WT and *Nlrp3*$^{-/-}$ animals displayed similar degrees of concentric cardiac hypertrophy with thickening of the septal diameter (Fig. 8*B*).

Consistent with previous reports, WT mice demonstrated diffuse, patchy fibrotic regions in the myocardium following AngII infusion, as determined by Masson trichrome staining (Fig. 8*C*). Specifically, AngII-treated WT hearts showed disruption of the myocardial interstitial architecture, with radiating reactive fibrosis projecting from perivascular structures. These regions were both less severe and largely reduced in *Nlrp3*$^{-/-}$ mice. Moreover, hearts from AngII-treated WT mice contained increased levels of collagen 1 and αSMA (Fig. 8*D*). We observed significantly reduced levels of these fibrotic markers in NLRP3-deficient, AngII-treated hearts, again supporting a role for NLRP3 in fibrotic signaling. Similar to these data, we also observed αSMA-expressing and FGF-2-positive cells in AngII-treated WT hearts, consistent with the proliferation and differentiation of resident cardiac interstitial cells toward the myofibroblast phenotype (Fig. 8*E*) (32). These regions were again both reduced and less severe in *Nlrp3*$^{-/-}$ hearts, further supporting the conclusion that NLRP3 regulates myofibroblast differentiation and fibrosis during cardiac injury.

Lastly, we looked to establish whether NLRP3 was also present in diseased human cardiac tissue. We collected human left ventricular tissue biopsies from five patients with end-stage heart disease that was complicated by varying degrees of long standing hypertension and ischemia at the time of left ventricular assist device surgical implantation. Consistent with our results from murine cardiac cells, we detected NLRP3 expression in the myocardium from all five samples, in addition to control left ventricular tissue from one patient without structural myocardial disease (Fig. 9*A*). Because chronically diseased cardiac tissue contains abundant and diverse cell types, we looked to directly visualize NLRP3 in human tissue specimens to further determine cellular expression profiles. In contrast to control myocardial tissue taken from patients without significant cardiac disease, failing human left ventricular tissue demonstrated prominent diffuse, radiating, and reactive fibrosis (Fig. 9*B*). These areas corresponded to highly collagenous regions containing cardiac myocytes with reduced titin organization, consistent with significantly impaired function (Fig. 9*C*). Importantly, we detected islands of NLRP3-expressing interstitial cells localized between damaged myocyte populations. These cells were largely absent from normal-appearing control myocardium and were surrounded by extracellular collagen, again supporting the conclusion that NLRP3 plays a role in cardiac myofibroblast signaling and fibrosis.

DISCUSSION

The differentiation of fibroblasts into myofibroblasts represents an important wound healing response during chronic injury (1). Recently, the NLR family of pattern recognition receptors has been characterized to mediate diverse aspects of wound healing through the regulation of proinflammatory cytokine products in professional immune cells (19). Although these processes are important determinants of the inflammatory response to ongoing injury, the role of NLR proteins in local resident cells such as cardiac fibroblasts is not completely understood. The unrestricted ability of fibroblasts to readily secrete potent cytokines, such as IL-1β, would give rise to significant immunopathology and collateral damage in the presence of even remote tissue stress. Mechanistically, additional roles for the NLRs in regulating the host defense independently from cytokine production during differential degrees of cellular stress are rational from a biological standpoint and would account for the observations that genetic deletion of NLRP3 confers protection in some animal models of heart and kidney

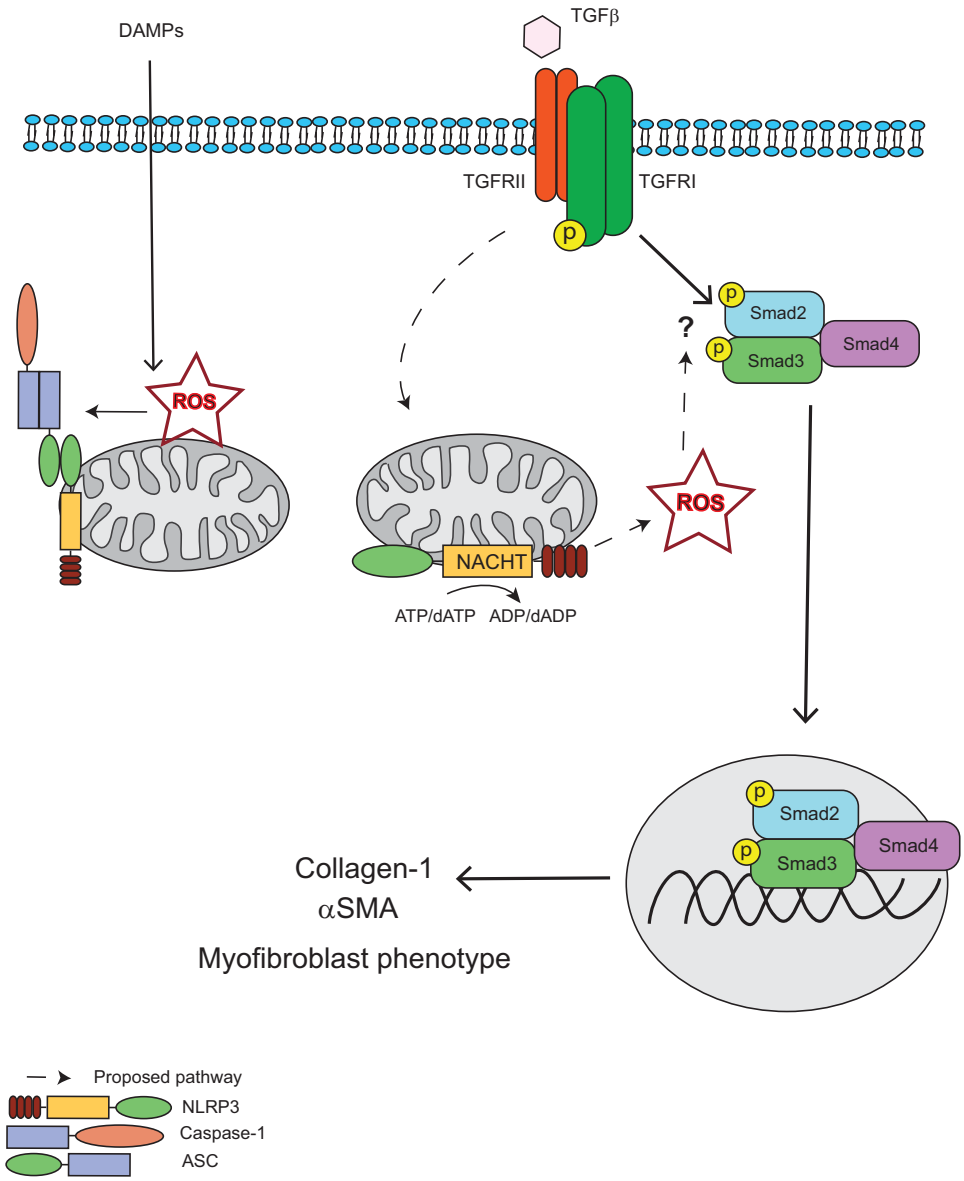

FIGURE 10. **Proposed mechanism for NLRP3 regulation of Smad signaling and fibrosis.** In response to TGFβ binding to the TGF receptor complex, NLRP3 augments the production of reactive oxygen species from the mitochondria, which act to promote R-Smad phosphorylation and subsequent nuclear accumulation through still uncharacterized mechanism. NLRP3-induced ROS production is dependent on the NACHT domain and ATP/dATP binding and hydrolysis. The phosphorylated active Smad2-Smad3-Smad4 transcription factor complex then translocates to the nucleus to induce Smad-dependent transcription and translation of profibrotic factors, such as collagen 1 and αSMA, resulting in a differentiation to the myofibroblast phenotype. *DAMP*, danger/damage-associated molecular pattern.

injury despite negligible IL-1β/IL-18 release (12, 24). Moreover, chimeric mice harboring deletion of NLRP3 restricted to the bone marrow are incompletely protected during renal injury models, supporting the importance of these proteins locally within solid organ systems (15). We have reported previously that NLRP3 in renal epithelial cells regulates TGFβ -induced epithelial mesenchymal transition independently from the inflammasome, suggesting a more general role for NLRP3 beyond cytokine regulation during chronic injury (14). Here we elaborate on those findings in cardiac fibroblasts to reveal the molecular determinants of the underlying response and confirm the *in vivo* relevance in a model of cardiac fibrosis. Our results establish a novel paradigm for NLRP3 in the fine-tuning of cellular differentiation and confirm the importance of NLRP3 in fibrosis and cardiac remodeling described previously by others. In addition to regulating inflammation and cytokine maturation, we propose a novel mechanism whereby NLRP3 modulates ROS production from the mitochondria to augment Smad signaling, fibrotic gene expression, and, ultimately, the phenotypic consequences of chronic disease (Fig. 10).

Reports on NLRP3 signaling in both professional and non-professional immune cells consistently describe relation to mitochondrial function. NLRP3 has been described to target mitochondria on activation of innate immune cells during inflammasome assembly (28). Others have recently proposed the presence of a putative mitochondrial localization signal, targeting NLRP3 from the cytoplasm to mitochondrial membranes in macrophages (27). Our results in primary human CFs

indicate that endogenous NLRP3 is, at least in part, associated constitutively with the mitochondria because we did not observe translocation during stimulation or disruption of mitochondrial integrity. Because the expression of NLRP3 in CFs is significantly lower than in innate immune cells, differential localization patterns could be a result of altered levels of gene expression. Alternatively, the presence or absence of binding proteins or molecular chaperones could also impact cellular distribution. The possibility also remains that the absolute degree of NLRP3 expression determines its functional ability to form an inflammasome or participate in non-canonical signaling. Further experiments are required to delineate the molecular determinants governing inflammasome-dependent and -independent processes in diverse cell types.

Although we found myofibroblast differentiation to occur independently from caspase 1 and IL-1β activation, the molecular biology of NLRP3 in augmenting Smad signaling was found to be similar to regulation of the inflammasome. We observed that only the NACHT domain was required for induction of R-Smads, whereas PYD and LRR were dispensable. In macrophages, similar structural results have been found in regulating the activation of caspase 1 and secretion of IL-1β, suggesting that nucleotide binding/hydrolysis and oligomerization are also important aspects in non-canonical NLRP3 responses (20). The NACHT domain is a complex structure containing at least seven conserved and distinct motifs (33). Its conservation in the NLR family implies structural relevance. Although we did not observe a complete reduction in NLRP3-induced R-Smad activation with Walker A mutant constructs, it is likely that other structural components are also important. Furthermore, although NLRP9 and NLRP10 failed to increase R-Smad activation compared with NLRP3, the role of other NLRs remains to be determined.

How NLRP3 functions at the mitochondria in cardiac fibroblasts to regulate ROS production and Smad signaling remains to be explored. TGFβ and AngII both induce mitochondrial ROS (30, 34, 35). Recent interest has surrounded the ability of mROS to induce Smad signaling and myofibroblast differentiation. However, a specific link has not yet been described. NLRP3 has been proposed previously to interact with members of the cellular redox machinery (28). It is plausible that similar interactions are also capable of regulating ROS levels from mitochondria. Indeed, other NLRs have been shown previously to proceed through similar paradigms. The atypical NLRX1, for example, is targeted to the mitochondrial matrix via an N-terminal-addressing sequence, where it regulates NFκB and JNK signaling following ROS promotion (36, 37). Our results for NLRP3 in cardiac fibroblasts appear to be similar. Thus, a dual function for NLRP3 both upstream and downstream of ROS may exist in diverse cell types to fine-tune inflammation and other cellular signaling processes involved in chronic injury.

In conclusion, we identified a novel role for NLRP3 in the development of cardiac fibrosis through its involvement in cardiac myofibroblast differentiation. Our findings suggest that NLRP3 is not intrinsically linked to the inflammasome but, rather, exerts distinct roles in response to injurious signals to regulate tissue homeostasis.

REFERENCES

1. van den Borne, S. W., Diez, J., Blankesteijn, W. M., Verjans, J., and Hofstra, L. (2010) Myocardial remodeling after infarction: the role of myofibroblasts. *Nat. Rev. Cardiol.* **7,** 30–37
2. Petrov, V. V, Fagard, R. H., and Lijnen, P. J. (2002) Stimulation of collagen production by transforming growth factor-B1 during differentiation of cardiac fibroblasts to myofibroblasts. *Hypertension* **39,** 258–263
3. Di Guglielmo, G. M., Le Roy, C., Goodfellow, A. F., and Wrana, J. L. (2003) Distinct endocytic pathways regulate TGF-β receptor signalling and turnover. *Nat. Cell Biol.* **5,** 410–421
4. Xu, L., Chen, Y. G., and Massagué, J. (2000) The nuclear import function of Smad2 is masked by SARA and unmasked by TGFβ-dependent phosphorylation. *Nat. Cell Biol.* **2,** 559–562
5. Wrana, J. L., Attisano, L., Wieser, R., Ventura, F., and Massagué, J. (1994) Mechanism of activation of the TGFβ receptor. *Nature* **370,** 341–347
6. Wang, W., Huang, X. R., Canlas, E., Oka, K., Truong, L. D., Deng, C., Bhowmick, N. A., Ju, W., Bottinger, E. P., and Lan, H. Y. (2006) Essential role of Smad3 in angiotensin II-induced vascular fibrosis. *Circ. Res.* **98,** 1032–1039
7. Yang, F., Huang, X. R., Chung, A. C., Hou, C. C., Lai, K. N., and Lan, H. Y. (2010) Essential role for Smad3 in angiotensin II-induced tubular epithelial-mesenchymal transition. *J. Pathol.* **221,** 390–401
8. Martinon, F., Burns, K., and Tschopp, J. (2002) The inflammasome: a molecular platform triggering activation of inflammatory caspases and processing of proIL-1β. *Mol. Cell* **10,** 417–426
9. Martinon, F., Mayor, A., and Tschopp, J. (2009) The inflammasomes: guardians of the body. *Annu. Rev. Immunol.* **27,** 229–265
10. Martinon, F., Pétrilli, V., Mayor, A., Tardivel, A., and Tschopp, J. (2006) Gout-associated uric acid crystals activate the NALP3 inflammasome. *Nature* **440,** 237–241
11. Vandanmagsar, B., Youm, Y. H., Ravussin, A., Galgani, J. E., Stadler, K., Mynatt, R. L., Ravussin, E., Stephens, J. M., and Dixit, V. D. (2011) The NLRP3 inflammasome instigates obesity-induced inflammation and insulin resistance. *Nat. Med.* **17,** 179–188
12. Mezzaroma, E., Toldo, S., Farkas, D., Seropian, I. M., Van Tassell, B. W., Salloum, F. N., Kannan, H. R., Menna, A. C., Voelkel, N. F., and Abbate, A. (2011) The inflammasome promotes adverse cardiac remodeling following acute myocardial infarction in the mouse. *Proc. Natl. Acad. Sci. U.S.A.* **108,** 19725–19730
13. Sandanger, Ø., Ranheim, T., Vinge, L. E., Bliksøen, M., Alfsnes, K., Finsen, A. V., Dahl, C. P., Askevold, E. T., Florholmen, G., Christensen, G., Fitzgerald, K. A., Lien, E., Valen, G., Espevik, T., Aukrust, P., and Yndestad, A. (2013) The NLRP3 inflammasome is up-regulated in cardiac fibroblasts and mediates myocardial ischaemia-reperfusion injury. *Cardiovasc. Res.* **99,** 164–174
14. Wang, W., Wang, X., Chun, J., Vilaysane, A., Clark, S., French, G., Bracey, N. A., Trpkov, K., Bonni, S., Duff, H. J., Beck, P. L., and Muruve, D. A. (2013) Inflammasome-independent NLRP3 augments TGF-β signaling in kidney epithelium. *J. Immunol.* **190,** 1239–1249
15. Vilaysane, A., Chun, J., Seamone, M. E., Wang, W., Chin, R., Hirota, S., Li, Y., Clark, S. A., Tschopp, J., Trpkov, K., Hemmelgarn, B. R., Beck, P. L., and Muruve, D. A. (2010) The NLRP3 inflammasome promotes renal inflammation and contributes to CKD. *J. Am. Soc. Nephrol.* **21,** 1732–1744
16. Fedak, P. W., Bai, L., Turnbull, J., Ngu, J., Narine, K., Duff, H. J. (2012) Cell therapy limits myofibroblast differentiation and structural cardiac remodeling basic fibroblast growth factor-mediated paracrine mechanism. *Circ. Heart Fail.* **5,** 349–356
17. Bracey, N. A., Beck, P. L., Muruve, D. A., Hirota, S. A., Guo, J., Jabagi, H., Wright, J. R., Jr., Macdonald, J. A., Lees-Miller, J. P., Roach, D., Semeniuk, L. M., and Duff, H. J. (2013) The Nlrp3 Inflammasome promotes myocardial dysfunction in structural cardiomyopathy through IL-1β. *Exp. Physiol.* **98,** 462–472
18. Derynck, R., and Zhang, Y. E. (2003) Smad-dependent and Smad-independent pathways in TGF-B family signaling. *Nature* **425,** 577–584
19. Martinon, F., and Tschopp, J. (2005) NLRs join TLRs as innate sensors of pathogens. *Trends Immunol.* **26,** 447–454
20. Duncan, J. A., Bergstralh, D. T., Wang, Y., Willingham, S. B., Ye, Z., Zim-

mermann, A. G., and Ting, J. P. (2007) Cryopyrin/NALP3 binds ATP/dATP, is an ATPase, and requires ATP binding to mediate inflammatory signaling. *Proc. Natl. Acad. Sci. U.S.A.* **104,** 8041–8046
21. Gasse, P., Mary, C., Guenon, I., Noulin, N., Charron, S., Schnyder-Candrian, S., Schnyder, B., Akira, S., Quesniaux, V. F., Lagente, V., Ryffel, B., and Couillin, I. (2007) IL-1R1/MyD88 signaling and the inflammasome are essential in pulmonary inflammation and fibrosis in mice. *J. Clin. Invest.* **117,** 3786–3799
22. Artlett, C. M., Sassi-Gaha, S., Rieger, J. L., Boesteanu, A. C., Feghali-Bostwick, C. A., and Katsikis, P. D. (2011) The inflammasome activating caspase 1 mediates fibrosis and myofibroblast differentiation in systemic sclerosis. *Arthritis Rheum.* **63,** 3563–3574
23. Zhang, H. Y., Gharaee-Kermani, M., and Phan, S. H. (1997) Regulation of lung fibroblast α-Smooth muscle actin expression, contractile phenotype, and apoptosis by IL-1β. *J. Immunol.* **158,** 1393–1399
24. Shigeoka, A. A., Mueller, J. L., Kambo, A., Mathison, J. C., King, A. J., Hall, W. F., Correia Jda, S., Ulevitch, R. J., Hoffman, H. M., and McKay, D. B. (2010) An inflammasome-independent role for epithelial-expressed Nlrp3 in renal ischemia-reperfusion injury. *J. Immunol.* **185,** 6277–6285
25. Zuurbier, C. J., Jong, W. M., Eerbeek, O., Koeman, A., Pulskens, W. P., Butter, L. M., Leemans, J. C., and Hollmann, M. W. (2012) Deletion of the innate immune NLRP3 Receptor abolishes cardiac ischemic preconditioning and is associated with decreased Il-6/STAT3 signaling. *PLoS ONE* **7,** e40643
26. Kayagaki, N., Warming, S., Lamkanfi, M., Vande Walle, L., Louie, S., Dong, J., Newton, K., Qu, Y., Liu, J., Heldens, S., Zhang, J., Lee, W. P., Roose-Girma, M., and Dixit, V. M. (2011) Non-canonical inflammasome activation targets caspase-11. *Nature* **479,** 117–121
27. Subramanian, N., Natarajan, K., Clatworthy, M. R., Wang, Z., and Germain, R. N. (2013) The adaptor MAVS promotes NLRP3 mitochondrial localization and inflammasome activation. *Cell* **153,** 348–361
28. Zhou, R., Tardivel, A., Thorens, B., Choi, I., and Tschopp, J. (2010) Thioredoxin-interacting protein links oxidative stress to inflammasome activation. *Nat. Immunol.* **11,** 136–140
29. Sena, L. A., and Chandel, N. S. (2012) Physiological roles of mitochondrial reactive oxygen species. *Mol. Cell* **48,** 158–167
30. Jain, M., Rivera, S., Monclus, E. A., Synenki, L., Zirk, A., Eisenbart, J., Feghali-Bostwick, C., Mutlu, G. M., Budinger, G. R., and Chandel, N. S. (2013) Mitochondrial reactive oxygen species regulate transforming growth factor signaling. *J. Biol. Chem.* **288,** 770–777
31. Koitabashi, N., Danner, T., Zaiman, A. L., Pinto, Y. M., Rowell, J., Mankowski, J., Zhang, D., Nakamura, T., Takimoto, E., and Kass, D. A. (2011) Pivotal role of cardiomyocyte TGF-β signaling in the murine pathological response to sustained pressure overload. *J. Clin. Invest.* **121,** 2301–2312
32. Matsui, Y., Ikesue, M., Danzaki, K., Morimoto, J., Sato, M., Tanaka, S., Kojima, T., Tsutsui, H., and Uede, T. (2011) Syndecan-4 prevents cardiac rupture and dysfunction after myocardial infarction. *Circ. Res.* **108,** 1328–1339
33. Leipe, D. D., Koonin, E. V., and Aravind, L. (2004) STAND, a class of P-loop NTPases including animal and plant regulators of programmed cell death: multiple, complex domain architectures, unusual phyletic patterns, and evolution by horizontal gene transfer. *J. Mol. Biol.* **343,** 1–28
34. Zhang, G. X., Lu, X. M., Kimura, S., and Nishiyama, A. (2007) Role of mitochondria in angiotensin II-induced reactive oxygen species and mitogen-activated protein kinase activation. *Cardiovasc. Res.* **76,** 204–212
35. Zimmerman, M. C., Lazartigues, E., Lang, J. A., Sinnayah, P., Ahmad, I. M., Spitz, D. R., and Davisson, R. L. (2002) Superoxide mediates the actions of angiotensin II in the central nervous system. *Circ. Res.* **91,** 1038–1045
36. Tattoli, I., Carneiro, L. A., Jéhanno, M., Magalhaes, J. G., Shu, Y., Philpott, D. J., Arnoult, D., and Girardin, S. E. (2008) NLRX1 is a mitochondrial NOD-like receptor that amplifies NF-κB and JNK pathways by inducing reactive oxygen species production. *EMBO Rep.* **9,** 293–300
37. Arnoult, D., Soares, F., Tattoli, I., Castanier, C., Philpott, D. J., and Girardin, S. E. (2009) An N-terminal addressing sequence targets NLRX1 to the mitochondrial matrix. *J. Cell Sci.* **122,** 3161–3168